

1 **Modeling the Enceladus Plume–Plasma Interaction**

B. L. Fleshman

2 Laboratory for Atmospheric and Space Physics, University of Colorado,

3 Boulder, Colorado, USA

4 Department of Physics and Astronomy, University of Oklahoma, Norman,

5 Oklahoma, USA

P. A. Delamere

6 Laboratory for Atmospheric and Space Physics, University of Colorado,

7 Boulder, Colorado, USA

F. Bagenal

8 Laboratory for Atmospheric and Space Physics, University of Colorado,

9 Boulder, Colorado, USA

Bobby Fleshman, Department of Physics and Astronomy, University of Oklahoma, 440 W.

Brooks, Norman, Oklahoma 73019, USA (fleshman@nhn.ou.edu)

arXiv:1001.0787v1 [astro-ph.EP] 5 Jan 2010

10 We investigate the chemical interaction between Saturn's corotating plasma
11 and Enceladus' volcanic plumes. We evolve a parcel of ambient plasma as
12 it passes through a prescribed H₂O plume using a physical chemistry model
13 adapted for water-group reactions. The flow field is assumed to be that of
14 a plasma around an electrically-conducting obstacle centered on Enceladus
15 and aligned with Saturn's magnetic field, consistent with Cassini magnetome-
16 ter data. We explore the effects on the physical chemistry due to: (1) a small
17 population of hot electrons; (2) a plasma flow decelerated in response to the
18 pickup of fresh ions; (3) the source rate of neutral H₂O. The model confirms
19 that charge exchange dominates the local chemistry and that H₃O⁺ dom-
20 inates the water-group composition downstream of the Enceladus plumes.
21 We also find that the amount of fresh pickup ions depends heavily on both
22 the neutral source strength and on the presence of a persistent population
23 of hot electrons.

1. Introduction

24 Early Cassini encounters with Enceladus revealed surprising evidence of a significant
 25 source of water (with trace percentages of other neutrals, including CO₂) from geysers
 26 located at the moon's southern pole [*Hansen et al.*, 2006; *Porco et al.*, 2006; *Spencer*
 27 *et al.*, 2006; *Waite et al.*, 2006]. The H₂O cloud reacts with Saturn's corotating plasma
 28 torus, loading Saturn's magnetosphere with fresh ions. The pickup rate \dot{M} quantifies
 29 the amount of fresh ions added to the magnetosphere from charge exchange and im-
 30 pact/photoionization. Respective contributions to pickup from charge exchange and im-
 31 pact/photoionization are fundamentally different in that charge exchange does not con-
 32 tribute to ion production because one ion replaces another. Both processes however
 33 introduce slow-moving ions which must subsequently be accelerated by Saturn's magne-
 34 tosphere.

35 Early identification of the interaction between the local water source and Saturn's coro-
 36 tating plasma was made by *Dougherty et al.* [2006]. Based on the Cassini Plasma Spec-
 37 trometer (CAPS, *Young et al.* [2004]) analysis by *Tokar et al.* [2006], *Pontius and Hill*
 38 [2006] modeled the interaction and derived a pickup rate of $\dot{M} \approx 100 \text{ kg s}^{-1}$. *Khurana*
 39 *et al.* [2007] and *Saur et al.* [2008] (hereafter K07 and S08) discovered a range in \dot{M}
 40 (0.2–3 kg s⁻¹) from Cassini magnetometer data in the three earliest Cassini Enceladus
 41 flybys (E0, 17 February 2005; E1, 09 March, 2005; E2, 14 July 2005). Constrained by Ion
 42 Neutral Mass Spectrometer (INMS, *Waite et al.* [2006]) and Ultraviolet Imaging Spectro-
 43 graph (UVIS, *Hansen et al.* [2006]) observations, *Burger et al.* [2007] estimated a pickup
 44 rate of $\dot{M} \approx 2\text{--}3 \text{ kg s}^{-1}$ from a neutral cloud model. The large discrepancy between

the pickup rates derived from CAPS and magnetometer data is due not only to the fact that the region considered by *Pontius and Hill* [2006] is much larger than that considered by K07 and S08, but also because the *Pontius and Hill* [2006] result depends on the poorly-constrained value of Saturn’s Pederson conductivity.

In this paper, we use a physical chemistry model to investigate the chemical interaction between the corotating plasma and the Enceladus plumes. Charge exchange dominates the local chemistry and leads to an H_3O^+ -dominated plasma downstream of Enceladus. We find that pickup increases when hot electrons are present—more so with a high neutral source rate.

2. Model

We use a physical chemistry model developed to study the Enceladus torus [*Delamere and Bagenal*, 2003; *Delamere et al.*, 2007; *Fleshman et al.*, 2009] to investigate the composition of plasma traveling along prescribed flow lines. The model evaluates mass and energy rate equations for water-group ions ($\text{W}^+ \equiv \text{O}^+ + \text{OH}^+ + \text{H}_2\text{O}^+ + \text{H}_3\text{O}^+$), protons, and thermal electrons in a parcel of plasma transiting the simulation. Neutrals are assumed to be cold, and in this study neutral abundances are fixed. The full set of reactions includes charge exchange, photoionization, ionization by electron impact, radiative excitation, recombination, and molecular dissociation by both electron impact and recombination. All species have isotropic Maxwellian speed distributions, and energy is transferred between species *via* Coulomb collisions. The simulation spans a rectangular domain extending $5 R_E$ from Enceladus in all directions except south, where the simulation extends to $15 R_E$ ($R_E = 252 \text{ km}$ is the radius of Enceladus).

66 A second population of supra-thermal ‘hot’ electrons is imposed with a fixed density
 67 (0.3 cm^{-3}) and temperature (160 eV). Hot electrons near Enceladus have been reported
 68 by *Tokar et al.* [2009] and have been observed throughout the torus by CAPS and the
 69 Radio and Plasma Wave Science Instrument [*Moncuquet et al.*, 2005; *Young et al.*, 2005].
 70 We showed in *Fleshman et al.* [2009] that a small amount of hot electrons is necessary to
 71 obtain the ambient ionization. Here we investigate the importance of hot electrons near
 72 Enceladus itself.

73 **Neutral source:** Following S08, the plume is prescribed as

$$74 \quad \frac{n_{\text{H}_2\text{O}}(r, \theta)}{n_0} = \left(\frac{R_E}{r}\right)^2 \exp \left[- \left(\frac{\theta}{H_\theta}\right)^2 - \left(\frac{r - R_E}{H_d}\right) \right], \quad (1)$$

75 where $H_\theta = 12^\circ$ and $H_d = 948 \text{ km}$ ($4 \times$ the Hill radius). S08 offset the plume from
 76 Enceladus’ southern pole by 8° and considered more than one source with the form of
 77 (1). We consider a single source whose origin coincides with Enceladus’ south pole. In
 78 the nominal case, n_0 is set to $2.5 \times 10^9 \text{ cm}^{-3}$, corresponding to a neutral source rate of
 79 $\approx 200 \text{ kg s}^{-1}$ (S08). S08 found a much stronger source for E0, so we also investigate the
 80 implications of a source with $n_0 = 2.2 \times 10^{10} \text{ cm}^{-3}$, corresponding to a neutral source rate
 81 of $\approx 1600 \text{ kg s}^{-1}$.

82 **Plasma flow field:** Because of the low Alfvén Mach number at Enceladus ($M_A \approx$
 83 0.1 , *Sittler et al.* [2008]), perturbations travel rapidly along the magnetic field so that the
 84 source region presents a cylindrical obstacle to the corotating plasma. We adopt the flow
 85 field used by *Dols et al.* [2008] to study the plasma interaction with Jupiter’s moon Io:

$$86 \quad \frac{\mathbf{u}}{v_{\text{amb}}} = \left[1 - \frac{\cos(2\phi)}{(\rho/R_E)^2} \right] \hat{\mathbf{x}} - \frac{\sin(2\phi)}{(\rho/R_E)^2} \hat{\mathbf{y}}, \quad (2)$$

87 where $v_{\text{amb}} \approx 0.8 \times v_{\text{cor}}$ ($v_{\text{cor}} \approx 26 \text{ km s}^{-1}$) is the ambient plasma speed far from Enceladus
 88 [*Wilson et al.*, 2009]. The magnetic field defines the z -axis and ϕ is measured from the
 89 flow direction.

90 Along each flow line, parcels of plasma were started $5 R_E$ upstream of Enceladus with
 91 the steady-state composition given in *Fleshman et al.* [2009]. The plasma was moved in
 92 the direction of the plasma flow to $5 R_E$ downstream, and the chemistry was updated
 93 at associated time steps. The pickup energy—determined by the relative speed between
 94 neutrals and plasma flow—was also updated. Ions far from Enceladus are picked up at
 95 v_{amb} , while those near Enceladus are picked up more slowly up- and downstream and more
 96 rapidly on the flanks.

97 To investigate the effect of ion pickup, we slowed the flow near the obstacle. We followed
 98 *Dols et al.* [2008] by decreasing the component of the plasma velocity in the flow direction:
 99 u_x was replaced by $\gamma(\rho)u_x$, where $\gamma(1 R_E) = 0.5$, increasing linearly to $\gamma(2 R_E) = 1$. We
 100 find however that a stronger slowing factor ($\gamma(1 R_E) = 0.1$) does not qualitatively change
 101 our results. In Section 3, we compare the pickup rates both for when the plasma has
 102 (nominal case) and has not been slowed.

103 Two effects are due directly to the slowing of the flow. First, the pickup energy is
 104 reduced, affecting the plasma temperature because fresh ions are picked up at the local
 105 plasma speed. Second, impact ionization increases because plasma transits more slowly.
 106 Impact ionization contributes directly to pickup, as well as indirectly, by seeding multiple
 107 charge exchanges.

108 We neglect gyromotion on the basis of scale. For example, an H_3O^+ ion picked up at v_{amb}
 109 has a gyroradius of only $0.1 R_E$. More important is that (in the frame of Enceladus) ions
 110 oscillate between zero and twice their pickup speed and we ignore the velocity dependence
 111 of charge exchange. Including gyromotion would enhance the effects we report in this
 112 paper.

113 **Hot electrons:** We estimate that hot electrons cool rapidly near the dense plume *via*
 114 impact ionization, and thus imposed a discontinuity at $\rho = 3 R_E$:

$$115 \quad n_{\text{eh}}/(\text{cm}^{-3}) = \begin{cases} 0 & 1 < \rho/R_E < 3 \\ 0.3 & 3 < \rho/R_E. \end{cases} \quad (3)$$

116 However, *Dols et al.* [2008] showed that field-aligned electron beams (perhaps associated
 117 with the Io auroral footprint) are necessary to model the high plasma density in Io's
 118 wake. At Enceladus, hot electrons may also be related to weak UV auroral spots recently
 119 observed by UVIS (W. Pryor, personal comm.). To investigate the implication of hot
 120 electrons at Enceladus, we consider the additional case where n_{eh} is held at 0.3 cm^{-3}
 121 throughout the simulation domain. The pickup rates for each case are compared in Section
 122 3.

123 **Pickup rate calculation:** Fresh ions are added to the magnetosphere by both charge
 124 exchange ($\dot{\rho}_{\text{exch}}$) and impact/photoionization ($\dot{\rho}_{\text{ioz}}$):

$$125 \quad \dot{\rho}_{\text{ioz}} = \sum_j n_e n_j m_j \kappa_j^{\text{imp}} + \sum_k n_k m_k \kappa_k^{\text{phot}} \quad (4)$$

$$126 \quad \dot{\rho}_{\text{exch}} = \sum_j n_j^{(1)} n_j^{(2)} m_j \kappa_j^{\text{exch}}. \quad (5)$$

128 The reaction rates (*Fleshman et al.* [2009]) are represented by κ^{imp} , κ^{exch} [$\text{cm}^3 \text{ s}^{-1}$], and
 129 κ^{phot} [s^{-1}]; the ion masses by m ; and $n^{(1)}$, $n^{(2)}$ are the charge-exchanging neutral and ion
 130 densities. Summations are carried out over processes involving the creation of fresh ions.

131 We calculated the time-averages of (4) and (5) to find the average pickup rates for
 132 plasma parcels migrating along each flow line and multiplied by the flow line volume
 133 to find the pickup rate for each flow line. The total pickup rate for each process was
 134 determined by summing the contribution from all flow lines throughout the simulation.

3. Results

135 We consider the x - y plane $7.5 R_E$ south of the center of Enceladus. For this, the nominal
 136 case, hot electrons exist throughout the domain, the neutral source rate is $\approx 200 \text{ kg s}^{-1}$,
 137 and the plasma is slowed in the flow direction (Section 2). The pickup energy, heavy-to-
 138 light ion abundance (W^+/H^+), H_3O^+/W^+ , and H_3O^+ temperature ($T_{H_3O^+}$) in this plane
 139 are shown in Figure 1. The obstacle is plotted in black and 18 flow lines are over-plotted
 140 and labeled. Composition and temperatures along this line are plotted in Figure 2, where
 141 the corresponding flow lines are indicated.

142 The H_3O^+ ion is the most abundant ion in the wake—a consequence explained by
 143 the importance of charge exchange and the fact that charge exchanges lead to H_3O^+
 144 in the presence of an abundant water source. All charge exchanges with H_2O in our
 145 model ultimately lead to either H_3O^+ or H_2O^+ by $H_2O^+ + H_2O \rightarrow H_2O + H_2O^+$ and
 146 $H_2O^+ + H_2O \rightarrow OH + H_3O^+$. The former reaction supports H_2O^+ density somewhat,
 147 but the H_2O^+ products also feed into the latter, producing H_3O^+ . The W^+/H^+ ratio
 148 increases rapidly because protons are removed by $H^+ + H_2O \rightarrow H + H_2O^+$. The increase
 149 in electron density is due mainly to impact ionization of the plume by hot electrons.

150 In Figure 2, the electron temperature has been normalized to the ambient electron
 151 temperature (2 eV), and the ion temperatures have been normalized to their respective

152 ambient pickup energies (1.5 and 29 eV). Protons and H_3O^+ bear the signature of the
 153 cooler pickup temperature from where they were created by charge exchange. A factor of
 154 a few decrease in ion temperature through Enceladus' wake has recently been observed
 155 by *Tokar et al.* [2009]. The electron temperature has also been cooled by a factor of 2.

156 **Pickup rate:** We calculated individually (Section 2) the mass of fresh ions picked
 157 up *via* charge exchange, \dot{M}_{exch} , and \dot{M}_{ioz} —the ratio of which illustrates the importance
 158 of charge exchange over impact ionization. The simulation was run for the eight cases
 159 shown in Table 1. The flow-field, hot-electron, and source-rate treatments are described
 160 in Section 2. We discuss the cases corresponding to a ‘weak’ 200 kg s^{-1} source (Cases
 161 1a–4a) and a ‘strong’ 1600 kg s^{-1} source (Cases 1b–4b) separately.

162 *Weak source (Cases 1a–4a):* When hot electrons exist locally (1a/2a), the total pickup is
 163 roughly 0.3 kg s^{-1} with a 40% increase when the plasma is slowed. Because of the longer
 164 occupation time associated with the slowed flow, hot electrons increase seed ionization
 165 (\dot{M}_{ioz}), and in turn increase charge exchange (\dot{M}_{exch}). When hot electrons are removed
 166 (3a/4a), \dot{M}_{ioz} decreases by a factor of 4, but \dot{M}_{exch} drops by $\approx 30\%$, implying that much
 167 of the pickup is occurring outside the cut-off point at $3 R_E$. Slowing the plasma has less
 168 effect in 3a than in 1a because longer occupation does not boost seed ionization without
 169 hot electrons.

170 *Strong source (Cases 1b–4b):* The effect of the hot electrons becomes more apparent
 171 with the strong source because a denser portion of the plume is intersected by the flow
 172 lines. The effect of slowing the plasma is similar to that in the weak-source case. The total
 173 pickup however is increased by a factor of 3 when comparing the cases with hot electrons

174 (1b/2b) to cases without (3b/4b). The almost linear response of the total pickup to \dot{M}_{ioz}
 175 (compare 1b/2b to 3b/4b) suggests that, unlike in the weak source case, most of the
 176 pickup is occurring inside the hot electron cutoff at $3 R_E$.

177 K07 and S08 were in rough agreement on the total pickup rate. For E1 and E2, they
 178 found $\approx 0.2\text{--}0.6 \text{ kg s}^{-1}$, and for E0 they found $\approx 3 \text{ kg s}^{-1}$. Because our model relies on
 179 a physical chemistry calculation alone, it is remarkable to have obtained the same pickup
 180 rates using neutral plume distributions similar to those in S08 (E0: strong source, E1 and
 181 E2: weak source).

182 Charge exchange dominates the chemistry by at least a factor of 6 in all cases. Because
 183 of this, the water-group composition ratios (shown only for the nominal case) are quali-
 184 tatively unaffected. In particular, $\text{H}_3\text{O}^+/\text{W}^+$ always increases while O^+/W^+ , OH^+/W^+ ,
 185 and $\text{H}_2\text{O}^+/\text{W}^+$ always decrease in Enceladus' wake. The dominance of H_3O^+ elsewhere
 186 has been observed by CAPS during Cassini's orbital insertion period [Tokar *et al.*, 2006;
 187 Sittler *et al.*, 2008]. *Fleshman et al.* [2009] found that a steady-state, water-based Ence-
 188 ladus torus underestimates the H_3O^+ abundance seen in the CAPS data. Though few *new*
 189 ions are produced at Enceladus, the process that produces H_3O^+ may have an important
 190 effect on the large-scale torus composition. A more complete global model of the torus
 191 should include the effect of dense H_2O on Saturn's corotating plasma demonstrated in
 192 this paper.

4. Discussion and conclusions

193 To investigate the impact of hot electrons on the chemistry, we have chosen the simplest
 194 flow field possible with minimal perturbation by Enceladus. This flow is roughly consis-

195 tent with the compact source derived from magnetometer data (K07) but is much less
196 perturbed than the flow reported by *Tokar et al.* [2006]. Similarly, we have started with
197 a single symmetric plume oriented due-south. In future studies we will explore multiple
198 jets (S08), displaced sources (K07), and a minor spherically-symmetric global component
199 [*Burger et al.*, 2007].

200 Our findings are summarized below:

201 1. Charge exchange dominates the plume-plasma chemistry, confirming previous work
202 by *Burger et al.* [2007] and consistent with estimates by *Johnson et al.* [2006].

203 2. Charge exchange leads largely to an H_3O^+ -dominated wake, consistent with INMS
204 [*Cravens et al.*, 2009]. Reactions leading to H_3O^+ are well known in the comet community
205 [*Aikin*, 1974; *Haberli et al.*, 1997].

206 3. Comparing our pickup rates to those derived from the Cassini magnetometer (K07
207 and S08), INMS, and UVIS [*Burger et al.*, 2007], we find that a persistent source of hot
208 electrons may exist near Enceladus. If present, beams of hot electrons at Enceladus may
209 be related to the weak UV auroral spots recently observed by W. Pryor (personal comm.).

210 **Acknowledgments.** This work was supported under NESSF grant Planet09F-0036
211 and CDAP grant 06-CASS06-0062.

References

- 212 Aikin, A. C. (1974), Cometary coma ions, *Astrophys. J.*, , 193, 263–+, doi:10.1086/153156.
213 Burger, M. H., E. C. Sittler, R. E. Johnson, H. T. Smith, O. J. Tucker, and V. I. Shema-
214 tovich (2007), Understanding the escape of water from Enceladus, *Journal of Geophys-*

- 215 *ical Research (Space Physics)*, *112*, 6219–+, doi:10.1029/2006JA012086.
- 216 Cravens, T. E., R. L. McNutt, J. H. Waite, I. P. Robertson, J. G. Luhmann, W. Kasprzak,
217 and W.-H. Ip (2009), Plume ionosphere of Enceladus as seen by the Cassini ion and neu-
218 tral mass spectrometer, *Geophys. Res. Lett.*, , *36*, 8106–+, doi:10.1029/2009GL037811.
- 219 Delamere, P. A., and F. Bagenal (2003), Modeling variability of plasma conditions in
220 the Io torus, *Journal of Geophysical Research (Space Physics)*, *108*, 1276–+, doi:
221 10.1029/2002JA009706.
- 222 Delamere, P. A., F. Bagenal, V. Dols, and L. C. Ray (2007), Saturn’s neutral torus versus
223 Jupiter’s plasma torus, *Geophys. Res. Lett.*, , *34*, 9105–+, doi:10.1029/2007GL029437.
- 224 Dols, V., P. A. Delamere, and F. Bagenal (2008), A multispecies chemistry model of
225 Io’s local interaction with the Plasma Torus, *Journal of Geophysical Research (Space*
226 *Physics)*, *113*, 9208–+, doi:10.1029/2007JA012805.
- 227 Dougherty, M. K., K. K. Khurana, F. M. Neubauer, C. T. Russell, J. Saur, J. S. Leisner,
228 and M. E. Burton (2006), Identification of a Dynamic Atmosphere at Enceladus with
229 the Cassini Magnetometer, *Science*, *311*, 1406–1409, doi:10.1126/science.1120985.
- 230 Fleshman, B. L., P. A. Delamere, and F. Bagenal (2009), A Sensitivity Study of the
231 Enceladus Torus, *ArXiv e-prints*.
- 232 Haberli, R. M., M. R. Combi, T. I. Gombosi, D. L. de Zeeuw, and K. G. Powell (1997),
233 Quantitative Analysis of H₂O⁺ Coma Images Using a Multiscale MHD Model with
234 Detailed Ion Chemistry, *Icarus*, *130*, 373–386, doi:10.1006/icar.1997.5835.
- 235 Hansen, C. J., L. Esposito, A. I. F. Stewart, J. Colwell, A. Hendrix, W. Pryor, D. She-
236 mansky, and R. West (2006), Enceladus’ Water Vapor Plume, *Science*, *311*, 1422–1425,

237 doi:10.1126/science.1121254.

238 Johnson, R. E., H. T. Smith, O. J. Tucker, M. Liu, M. H. Burger, E. C. Sittler, and R. L.
239 Tokar (2006), The Enceladus and OH Tori at Saturn, *Astrophys. J.*, , *644*, L137–L139,
240 doi:10.1086/505750.

241 Khurana, K. K., M. K. Dougherty, C. T. Russell, and J. S. Leisner (2007), Mass loading
242 of Saturn’s magnetosphere near Enceladus, *Journal of Geophysical Research (Space*
243 *Physics)*, *112*, 8203–+, doi:10.1029/2006JA012110.

244 Moncuquet, M., A. Lecacheux, N. Meyer-Vernet, B. Cecconi, and W. S. Kurth
245 (2005), Quasi thermal noise spectroscopy in the inner magnetosphere of Saturn with
246 Cassini/RPWS: Electron temperatures and density, *Geophys. Res. Lett.*, , *32*, 20–+,
247 doi:10.1029/2005GL022508.

248 Pontius, D. H., and T. W. Hill (2006), Enceladus: A significant plasma source for Saturn’s
249 magnetosphere, *Journal of Geophysical Research (Space Physics)*, *111*, 9214–+, doi:
250 10.1029/2006JA011674.

251 Porco, C. C., et al. (2006), Cassini Observes the Active South Pole of Enceladus, *Science*,
252 *311*, 1393–1401, doi:10.1126/science.1123013.

253 Saur, J., N. Schilling, F. M. Neubauer, D. F. Strobel, S. Simon, M. K. Dougherty, C. T.
254 Russell, and R. T. Pappalardo (2008), Evidence for temporal variability of Enceladus’
255 gas jets: Modeling of Cassini observations, *Geophys. Res. Lett.*, , *35*, 20,105–+, doi:
256 10.1029/2008GL035811.

257 Sittler, E. C., et al. (2008), Ion and neutral sources and sinks within Saturn’s
258 inner magnetosphere: Cassini results, *Planetary Space Science*, *56*, 3–18, doi:

259 10.1016/j.pss.2007.06.006.

260 Spencer, J. R., et al. (2006), Cassini Encounters Enceladus: Background and the Discovery
261 of a South Polar Hot Spot, *Science*, *311*, 1401–1405, doi:10.1126/science.1121661.

262 Tokar, R. L., R. E. Johnson, M. F. Thomsen, R. J. Wilson, D. T. Young, F. J.
263 Crary, A. J. Coates, G. H. Jones, and C. S. Paty (2009), Cassini detection of Ence-
264 ladus' cold water-group plume ionosphere, *Geophys. Res. Lett.*, , *36*, 13,203–+, doi:
265 10.1029/2009GL038923.

266 Tokar, R. L., et al. (2006), The Interaction of the Atmosphere of Enceladus with Saturn's
267 Plasma, *Science*, *311*, 1409–1412, doi:10.1126/science.1121061.

268 Waite, J. H., et al. (2006), Cassini Ion and Neutral Mass Spectrometer: Enceladus Plume
269 Composition and Structure, *Science*, *311*, 1419–1422, doi:10.1126/science.1121290.

270 Wilson, R. J., R. L. Tokar, and M. G. Henderson (2009), Thermal ion flow in saturn's
271 inner magnetosphere measured by the cassini plasma spectrometer: A signature of the
272 enceladus torus?, *Geophys. Res. Lett.*, *36*.

273 Young, D. T., et al. (2004), Cassini Plasma Spectrometer Investigation, *Space Science*
274 *Reviews*, *114*, 1–4, doi:10.1007/s11214-004-1406-4.

275 Young, D. T., et al. (2005), Composition and Dynamics of Plasma in Saturn's Magneto-
276 sphere, *Science*, *307*, 1262–1266, doi:10.1126/science.1106151.

Case	kg s^{-1}	\dot{M}_{exch} ($10^{25} \text{ H}_2\text{O s}^{-1}$)	kg s^{-1}	\dot{M}_{ioz} ($10^{25} \text{ H}_2\text{O s}^{-1}$)	$\dot{M}_{\text{exch}}/\dot{M}_{\text{ioz}}$
(1a) Hot electrons + slowed flow	0.25	(0.84)	0.038	(0.13)	6.7
(2a) Hot electrons + un-slowed flow	0.22	(0.74)	0.034	(0.11)	6.6
(3a) No hot electrons + slowed flow	0.18	(0.61)	0.0091	(0.030)	20
(4a) No hot electrons + un-slowed flow	0.17	(0.58)	0.0087	(0.029)	20
(1b) Hot electrons + slowed flow	2.2	(7.3)	0.33	(1.1)	7.0
(2b) Hot electrons + un-slowed flow	1.9	(6.5)	0.30	(0.99)	6.6
(3b) No hot electrons + slowed flow	0.77	(2.6)	0.079	(0.26)	9.8
(4b) No hot electrons + un-slowed flow	0.77	(2.6)	0.076	(0.25)	10

Table 1. Pickup rates from charge exchange (\dot{M}_{exch}) and impact/photoionization (\dot{M}_{ioz}) for the eight cases discussed in the text. Only \dot{M}_{ioz} increases the plasma density (n_e). The cases labeled with ‘a’ correspond to a neutral source rate of 200 kg s^{-1} ; those labeled with ‘b’ correspond to a neutral source rate of 1600 kg s^{-1} . Case (1a), in bold, is the nominal case from which Figures 1 and 2 have been generated.

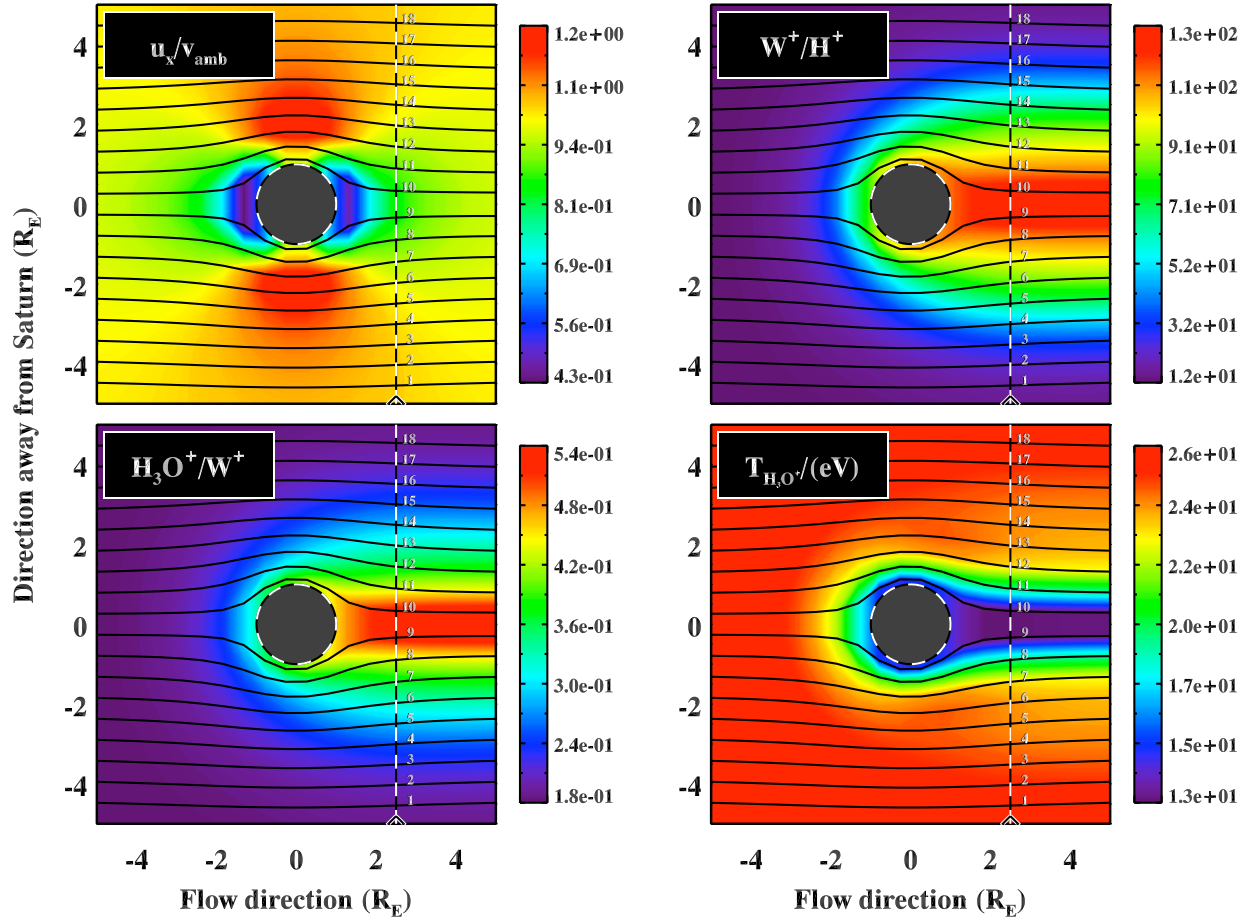


Figure 1. *Upper-left:* the x component of the assumed local plasma flow speed (Section 2) normalized to the ambient flow speed (80% of rigid corotation). *Upper-right:* water-group to proton abundance ratio. *Lower-left:* $\text{H}_3\text{O}^+/\text{W}^+$ abundance ratio. *Lower-right:* H_3O^+ temperature. The plane represented here is $7.5 R_E$ south of Enceladus. Model output along the dashed line is given in Figure 2.

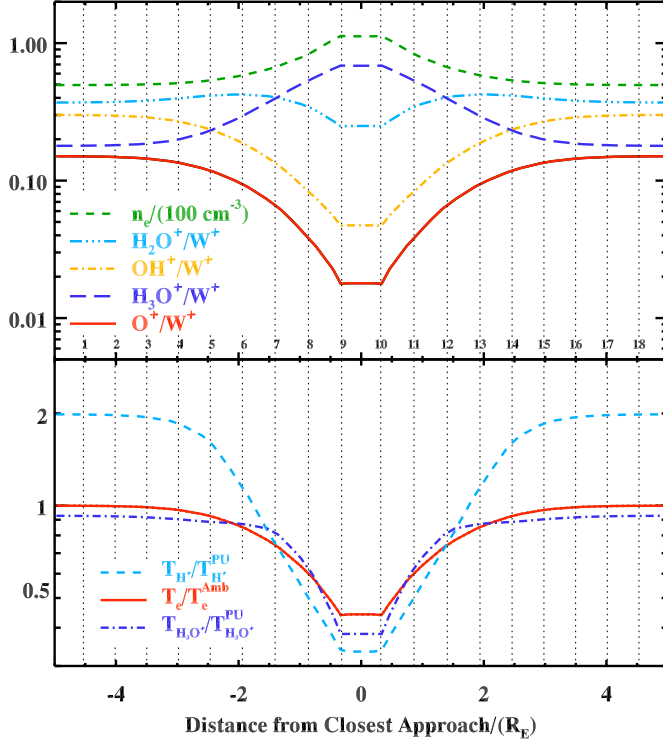


Figure 2. *Top:* Abundances and electron density from the simulation along the dashed line in Figure 1. *Bottom:* Electron, proton and H_3O^+ temperatures along the same cut. The electron temperature is normalized to its ambient temperature (2 eV), and the ion temperatures are normalized to their ambient pickup energies—1.5 and 29 eV for H^+ and H_3O^+ respectively.